DOI: 10.1002/ ((please add manuscript number))
Article type: Full Paper

# Relaxor Behavior in Ordered Lead Magnesium Niobate ($PbMg_{1/3}Nb_{2/3}O_3$) Thin Films

*Smitha Shetty[1*], Anoop Damodaran[2], Ke Wang[1], Yakun Yuan[1], Venkat Gopalan[1,4], Lane Martin[2,3] and Susan Trolier-McKinstry[1]*

[1]*Department of Materials Science and Engineering and Materials Research Institute, The Pennsylvania State University, PA*

[2]*Department of Materials Science and Engineering, University of California, Berkeley, CA*

[3]*Materials Sciences Division, Lawrence Berkeley National Laboratory, Berkeley, CA*

[4]*Department of Physics, and Department of Engineering Science and Mechanics, The Pennsylvania State University, PA*

Keywords: relaxor, short and long-range order, random site model, ferroelectricity, temperature dependent Rayleigh analysis

The local compositional heterogeneity associated with short-range ordering of Mg and Nb in $PbMg_{1/3}Nb_{2/3}O_3$ (PMN) is correlated with its characteristic relaxor ferroelectric behavior. Fully-

This is the author manuscript accepted for publication and has undergone full peer review but has not been through the copyediting, typesetting, pagination and proofreading process, which may lead to differences between this version and the Version of Record. Please cite this article as doi: 10.1002/adfm.201804258.

This article is protected by copyright. All rights reserved.

Author Manuscript

ordered PMN has not been prepared as a bulk material. This work examines the relaxor behavior in PMN thin films grown at temperatures below 1073 K by artificially reducing the degree of disorder via synthesis of heterostructures with alternate layers of $Pb(Mg_{2/3}Nb_{1/3})O_3$ and $PbNbO_3$, as suggested by the random-site model. 100-nm-thick, phase-pure films were grown epitaxially on (111) $SrTiO_3$ substrates using alternate target timed pulsed-laser deposition of $Pb(Mg_{2/3}Nb_{1/3})O_3$ and $PbNbO_3$ targets with 20% excess Pb. Selected area electron diffraction confirmed the emergence of (1/2, 1/2, 1/2) superlattice spots with randomly distributed ordered domains as large as ~150 nm. These heterostructures exhibited a dielectric constant of 800, loss tangents of ~0.03 and 2 x remanent polarization of ~11 $\mu C/cm^2$ at room temperature. Polarization-electric field hysteresis loops, Rayleigh data, and optical second-harmonic generation measurements are consistent with the development of ferroelectric domains below 140 K. Temperature-dependent permittivity measurements demonstrate reduced frequency dispersion compared to short range ordered PMN films. This work suggests a continuum between normal and relaxor ferroelectric behavior in the engineered PMN thin films.

Author Manuscript

## 1. Introduction

Lead magnesium niobate ($PbMg_{1/3}Nb_{2/3}O_3$) is a prototypical perovskite relaxor ferroelectric, known for its exceptional dielectric and electrostrictive properties, and valued for use in the actuators employed to control the corrector mirror tip and tilt in the Hubble telescope[1,2]. Furthermore, domain engineered PMN relaxor-$PbTiO_3$ single crystals possess strong piezoelectricity ($d_{33}$ > 2000 pC/N) and electromechanical coupling coefficients ($k_{33}$ > 0.9) [3]. Recent work by Li *et al.*[4,5] demonstrated that up to 80% of these exceptional properties are due to the alignment and

This article is protected by copyright. All rights reserved.

rotation of nanoscale inhomogeneities, known as polar nanoregions (PNRs), which are found in relaxors and arise due to intermediate range cation order.

However, the exact role of cation order in PMN has been the subject of considerable debate. The compositional heterogeneity associated with the lack of long-range ordering of the *B* cation sites in $Pb(B_{1/3}B'_{2/3})O_3$ is correlated with its characteristic relaxor behavior; this includes the dielectric dispersion below the maximum in permittivity as a function of temperature, and collapse of that dispersion at higher temperatures [6–8]. From a structural point of view, the average symmetry of PMN, when probed by conventional X-ray or neutron diffraction, appears to be cubic ($Pm\bar{3}m$) down to low temperatures with no evidence of a macroscopic structural-phase transition taking place through or below the temperature of maximum permittivity ($T_{max}$ = 265 K, at 1 kHz). However, diffuse scattering about the Bragg peaks has been observed below the Burns temperature $T_d$ (or $T_B$) ≈ 620 K, indicating the presence of local PNR with rhombohedral *R*3*m* symmetry dispersed in a non-polar matrix. The volume fraction of PNRs is reported to increase upon cooling to reach about 25 vol% at 5 K[8]. Such an evolution of ergodic local structure is in agreement with deviations from linearity of the refractive index, the lattice parameters, the thermal expansion, and strain and deviation of the dielectric permittivity from the Curie-Weiss law below $T_d$[7]. The mechanism responsible for dispersion in the relative permittivity is yet to be understood completely, though it is widely attributed to the dynamics of the PNRs. Several models have been proposed to explain this phenomenon: the paraelectric[2], dipolar glass[9,10], domain-like interface breathing[11–13], random-field[14], spherical-random-field, random-bond models[15], etc. Cross's superparaelectric model[7] considered the PNRs to be local regions with rhombohedral distortion, having polarization fluctuations/reorientations among equivalent <111> with anisotropic activation energies comparable to $k_bT$ at high temperature (where $k_b$ is Boltzmann's constant and T is temperature). The

This article is protected by copyright. All rights reserved.



Author Manuscript

size of the PNRs in bulk PMN increases near a characteristic freezing temperature $T_f$ (220 K), below which the material freezes into a static "glassy" state (nonergodic state with pseudocubic phase and isotropic properties) without long-range order, in the absence of an electric field. However, it has been reported that a dc electric field (>$E_{critical}$ = 1.7 kV/cm) can induce a ferroelectric transition from the glassy state in field-cooled[16,17], bulk PMN. In the same way, application of a dc bias field induces long range ferroelectric order in a zero-field-cooled sample, at 200 K, albeit in a longer time[18].

Furthermore, relaxors are characterized by the presence of compositionally-ordered regions (CORs) with short ordering lengths[19]. In contrast to PNRs, however, the morphology of CORs (their dimensions and the degree of compositional order) differs in different material systems with varying *B* site cations. Setter *et al*.[6] demonstrated that long-range ordering could be achieved in $PbSc_{1/2}Ta_{1/2}O_3$ (PST) ceramics (1:1 Sc:Ta order) by thermal annealing at 1273 K for 24 hrs. Well-ordered samples showed a normal ferroelectric transformation, while short range ordered samples were relaxor ferroelectrics. TEM analysis by Randall *et al*.[20] confirmed the increase in size of CORs from 2 nm in disordered as-sintered samples to ~200 nm in fully-ordered ceramics.

A fully-ordered state has not been achieved in PMN bulk ceramics or crystals. Long range 1:1 ordered domains have been coarsened in either $PbMg_{1/3}Ta_{2/3}O_3$ or doped-PMN ceramics, via heat treatments in the range of 1523-1623 K[21–24]. However, it was found that the ordering length in PMN was restricted to 2-6 nm, irrespective of extended thermal annealing times. Akbas *et al*.[25,26] proposed that PMN undergoes a thermodynamic order-to-disorder transition at temperatures below 1073 K. Thus, the short-range ordering in PMN may be a quenched representation of the high-temperature, disordered phase. This low ordering temperature kinetically restricts the development of the thermodynamically-stable, ordered phase as the material is cooled. Compared to $PbMg_{1/3}Ta_{2/3}O_3$ (where $T_{disorder}$ = 1648 K), the lower transition temperature for PMN was attributed to

This article is protected by copyright. All rights reserved.



Author Manuscript

higher covalency/polarizability of $Nb^{5+}$ compared to $Ta^{5+}$, and hence a reduced Coulombic driving force for order. Akbas and Davies[26,27] interpreted the short-range ordering using the charge-balanced "random-site" model.[28] This model suggests stacking of two sublattices in the CORs ($Pb\mathcal{B}'\mathcal{B}''O_3$) along [111]; the $\mathcal{B}''$sublattice (which contains only $Nb^{5+}$), alternates with the $\mathcal{B}'$ plane (a 2:1 random mixture of $Mg^{2+}$ and $Nb^{5+}$cations) for charge balance. This gives rise to doubling of the unit-cell size and an $Fm\bar{3}m$ space group inside the CORs. The net 1:2 Mg:Nb ratio in the CORs proposed by this model was experimentally confirmed by atomic resolution Z contrast imaging[29], and X-ray energy dispersive spectroscopy[30].

However, unlike PST, dielectric measurements showed the retention of relaxor behavior in thermally-coarsened domains in $PbMg_{1/3}Ta_{2/3}O_3$ and doped PMN. Two possible mechanisms can explain this anomaly: "random" fields[11,31] arising from chemical disorder either by charged defects like lead and oxygen vacancies and/or inherent disorder existing on the $\mathcal{B}'$ sublattice of the random-site model. Chu *et al*.[32,33] demonstrated a spontaneous relaxor to normal transition in *stoichiometric* short range ordered PST samples, while similar samples with < 3.5% lead vacancies retained relaxor characteristics. It is believed that the lead vacancies frustrate cooperative displacements of the sublattices. Interestingly, the CORs in short range ordered-PST samples with lead vacancies (< 3.5%) were larger than those in stoichiometric samples. This work suggests the possibility that PbO loss during long ordering anneals at 1473-1673 K in $PbMg_{1/3}Ta_{2/3}O_3$ or doped PMN can promote relaxor behavior, despite simultaneous coarsening of the CORs. Alternately, it can be hypothesized that the relaxor characteristics can be correlated to the atomic disorder[27] introduced by the random distribution of the $Mg^{2+}$ and $Ta^{5+}/Nb^{5+}$ ions on the $\mathcal{B}'$ lattice in the CORs in PMT/PMN systems. Chen *et al*.[33,34] modelled the influence of the size of *B*-site cations (Mg vs. Nb) on the $\mathcal{B}'$ sublattice on strengthening the long range order ferroelectric coupling. 1:1 order in adjacent sublattices was

Author Manuscript

This article is protected by copyright. All rights reserved.

reported to promote increased long-range coupling in the lattice, facilitating a relaxor-to-ferroelectric transition due to increased displacement of the $Pb^{2+}$ ion along the <111> towards the *B*' position[27]. This implies that relaxor behavior may persist even in *stoichiometric* $Pb(B_{1/3}B'_{2/3})O_3$ systems. There is a lack of experimental evidence to support the above assertion since fully-ordered, stoichiometric PMN-type materials have not been grown as bulk ceramics, though varying degrees of cation order have been achieved in a narrow window of kinetic activity and thermodynamic stability.

In addition, the relation between the PNRs, CORs, and the freezing of the PNRs leading to the non-ergodic phase in PMN is not clearly understood. At high temperature, the PNR clusters are small and non-interacting; however, on cooling below $T_B$, they can correlate with the neighboring clusters and grow in size (as controlled by the correlation length). Drawing an analogy with spin glasses, Viehland[9,35] demonstrated that the frequency dependence of the dielectric data could be fit with the Vogel-Fulcher relationship using a temperature-dependent correlation activation energy among PNR clusters, followed by freezing at $T_f$. This suggested the possibility that clusters could interact elastically through the rhombohedral distortion, as per the superparaelectric model. A long-range ordered ferroelectric state can be achieved if these clusters percolate (spontaneously[33] or under an applied electric field[17]). Burton's theoretical work using molecular dynamics based on first principles[36] in both PST and PMN proposed that the CORs act as nucleation centers for the PNRs. Local fields due to chemical disorder in the paraelectric matrix pin the PNRs from extending into the matrix, impeding the correlation between PNR clusters and leading to the glassy state in PMN. This could potentially imply that a completely-ordered matrix with minor defects in PMN could suppress the formation of PNRs or, at the very least, enable a spontaneous relaxor-to-normal-ferroelectric transition. Inelastic neutron scattering techniques[37] have demonstrated dampening of the transverse optic mode, a so called waterfall effect, when the material is cooled below $T_d$. However,

This article is protected by copyright. All rights reserved.



Author Manuscript

there is recovery of the TO mode at temperatures around 213 K. Though this ordering is not visible via X-ray measurements, nonlinear dielectric spectroscopy suggests a ferroelectric transition for field cooled PMN.

This paper aims to address the kinetic-growth limitation required to achieve a thermodynamically-stable, ordered state in PMN, via synthesis of thin PMN heterostructure films with ordered layers of stoichiometric $Pb[Mg_{2/3}Nb_{1/3}]O_3$ and $PbNbO_3$ grown at lower temperature ($<T_{order\text{-}disorder}$ = 1073 K). This is illustrated in the schematic in **Figure 1**. (111)-oriented films were grown on $SrTiO_3$ substrates with conducting $La_{0.7}Sr_{0.3}MnO_3$ bottom electrodes using timed pulsed-laser deposition. Without RHEED, it was not possible to get layer-by-layer growth in these relaxed films. That said, for any area on the surface, the fluxes were delivered with alternating compositions. This enabled growth of local long range ordered $Pb([Mg^{2+}_{2/3}Nb^{5+}_{1/3}]_{1/2}[Nb^{5+}]_{1/2})O_3$ regions in the film matrix with reduced relaxor-like behavior at length scales not achievable in bulk, while ensuring local lead stoichiometry. Though the relaxor behavior did not switch "off", this work has implications on understanding the impact of chemical ordering on polar domains in PMN. TEM characterization, supported by dielectric and second-harmonic generation measurements, suggests that the low-temperature state of these PMN heterostructures is ferroelectric with domains of tens of nanometer size, similar to the assertion made by Fu *et al*. in PMN single crystals[28]. With decreasing temperature, we speculate a continuum of ferroelectric and relaxor behavior, with increased percolating volume fraction of PNR in long range ordered PMN heterostructure films.

Author Manuscript

This article is protected by copyright. All rights reserved.

## 2. Results and Discussion

### 2.1. Structural Characterization

XRD patterns for the long range ordered PMN heterostructure and the short range ordered PMN films, grown on (001) and (111) STO substrates are shown in Figure 2(a). Phase pure perovskite films were obtained for growth on (111) substrates, while a niobium-rich second phase developed for films on (001) STO. Long range ordered PMN heterostructure films exhibited a full width half maximum of 0.1º in the ω rocking curves about the 111 reflection, as shown in the inset of Figure 2(b). Superstructure reflections of type (1/2 1/2 1/2) were not observed in the XRD pattern. This could be attributed to the incomplete ordering and/or length scale of the randomly distributed chemically ordered regions. Single target short range ordered PMN films were also found to be phase pure. PMN is relaxed at the grown thicknesses for both short-range and long-range films.

A TEM image [Figure 3(a)] and the fast Fourier transform (FFT) from the corresponding high resolution TEM image from the same region (Figure 3(b)) indicate epitaxial growth of the 100 nm thick PMN heterostructure on the 45 nm thick LSMO bottom electrode. No evidence of secondary phases was observed in the sample by TEM, in agreement with the XRD investigations. The dislocation density is not so high, though there are some edge dislocations at the interface; these dislocations are somewhat curved and appear without a fixed period. The FFT along the [-112] pole shows the (½ , ½, ½) superstructure reflections indicating cation ordering. The dark field images in Figure 3(c) and (d) were acquired using one of these superstructure reflections and show long range ordered domains as large as 150 nm (marked as a dotted region in the image). Fig 3(c) shows the chemically ordered regions are distributed in the heterostructure film (throughout the TEM sample size). Figure 4 (a) is a TEM image showing the cross-sectional structure of a short ordered PMN film

This article is protected by copyright. All rights reserved.



Author Manuscript

on LSMO/STO. In contrast, the FFT from the corresponding high resolution TEM image of the epitaxial PMN deposited from the single target shows diffuse superlattice reflections for chemical ordering, as expected. Additionally, in the dark field TEM data (Figure 4(c)), fewer ordered regions were observed with sizes less than 10 nm.

Figure 5 show the bright and dark field images of the same area imaged using the 111 reflection at room temperature and 100 K in situ, obtained during a heating cycle for the long range ordered PMN heterostructure. Figure 5(a) and (b) were collected at room temperature, while (c) and (d) were at 100 K. Clearly the microstructures are very different between these two temperatures. In the dark field images (Figure 5(d) and (e)) shown at 100K, a fringe-like contrast having a spacing of ~0.7 nm is seen in volumes with columnar shape. The long axis of those columnar regions is normal to the interface; the domains are ~10-20nm in size along the short axis and ~50 nm along the long axis. This observation is consistent with the polar microdomain imaging in the (110) orientation, reported in bulk PMN during heating[38,39]. These fine structures disappear as the film is heated beyond 220 K. These fringe-like structures are speculated to be a *result* of polar macrodomains of the rhombohedral phase, as suggested by previous work[38,39]. Based on the contrast from dark field, the volume fraction of the polar cluster was estimated to be ~20-30% at 100K. This volume fraction is above the theoretical prediction for geometrical percolation threshold[40] (18-20%) for ellipsoidal clusters with aspect ratio ranging from 1:5 to 1:2.5 and consistent with the neutron scattering pair distribution function analysis results at 15K by Jeong *et al*.[41]. This favors the prevalence of ferroelectric state in ordered PMN at low temperature.

**2.2. Electrical characterization**

The ferroelectric properties of the ordered PMN heterostructure film were studied by polarization – electric field (P-E) hysteresis loop measurements as a function of temperature. Slim,

This article is protected by copyright. All rights reserved.



Author Manuscript

but well-defined nested hysteresis loops were obtained, as shown in Figure 6a, with low levels of leakage. At room temperature, twice remanent polarization ($2P_r$) and coercive field ($E_c$) of the heterostructure PMN film were found to be -11.3 μC/cm$^2$ and -110 kV/cm, respectively. The polarization value is considerably higher than in previously reported work, presumably due to stabilization of the field-induced polarization as a consequence of the partial cation ordering achieved in the film. The ferroelectric behavior of the films was also confirmed by capacitance-field measurements; as shown in Figure 6b, the data show switching peaks that are the fingerprint of the ferroelectric switching. Increasing nonlinearity and hysteresis was observed in large signal P-E hysteresis loops as the temperature was lowered to 10 K. At low temperature, the loops became increasingly more square [Figure 6(c)]; on heating. the temperature dependence of the remanent polarization reveals a gradual loss in polarization with temperature which is consistent with relaxor characteristics.

Figure 7(a) and 7(b) show the temperature dependence of the relative dielectric constant and its loss at different frequencies, for 100 nm thick long range ordered and short range ordered PMN films. The long range ordered PMN heterostructure shows less dispersion of the permittivity, compared to that found in the short range ordered film. Shift in $T_{max}$ (compared at the highest and the lowest frequencies) in the case of short range ordered film is ~40 K, however in the case of long range ordered film, this difference is ~25 K. In the ordered film beyond $T_{max}$, the dielectric response converged while more space charge in the short range ordered film leads to a failure to converge the permittivity data above $T_{max}$. As expected, the maximum permittivity of the PMN thin film is much below that of bulk ceramics (~16,000), which is certainly due, at least in part to substrate clamping[42,43].

Author Manuscript

This article is protected by copyright. All rights reserved.

The relaxor behavior did not turn "off" completely in the ordered sample, despite observing increased size of chemically ordered regions in TEM. Electron diffraction is poor at distinguishing complete and partial ordering. Recent atomic resolution HAADF STEM imaging work by Lebeau et al.[44] demonstrated the presence of chemical order gradients within each COR in relaxor PMN, rather than abrupt transition between the COR and disordered matrix. Also, the order metric (defined as the standard deviation of the Mg/Nb atom column intensities surrounding each Pb/O atom column normalized to mean) is independent of the COR size in the ordering gradient model. Thus, relaxor behavior in PMN might be strongly influenced by the disorder inherent in the *B*' sublattice of the COR in the ordered PMN films. This random positional disorder cannot be controlled during growth and hence ordering along one dimension is not enough to turn off relaxor ferroelectricity. Our results assert a mixture of ferroelectric and relaxor behavior in the long range ordered PMN heterostructure films, as the ordering observed is inadequate to drive a fully ferroelectric state.

Figure 8(a) shows the effect of increasing ac field (3-25 kV/cm) as measured at 1 kHz on long range ordered PMN films, as a function of temperature. The permittivity increased linearly as a function of ac field, with $T_{max}$ shifting to lower temperature. These data were fitted using the Rayleigh law $\varepsilon_r = \varepsilon_{init} + \alpha E_{ac}$ for ac fiels up to ~1/3-1/2*coercive field. The irreversible Rayleigh coefficient $\alpha$ represents the irreversible movement of domain walls, polar cluster boundaries, or phase boundaries, while $\varepsilon_{init}$ arises from both the intrinsic response and reversible motion of boundaries. The Rayleigh coefficients decrease at higher frequencies, which would be consistent with observations by Glazunov et al.[45] in PMN single crystals. These data suggest a domain wall or interface boundary type relaxation phenomenon, instead of the thermally activated polarization

This article is protected by copyright. All rights reserved.



Author Manuscript

flips, as would have been suggested by the superparaelectric model. As observed in Figure 8(b), α peaked at 130-140 K for the heterostructure sample. The decrease in α at low temperatures is presumed to be due to loss of thermal activation of the mobile boundaries, as described by Li et al.[5] The decrease in α at high temperature is likely to be due to a reduction in the number of mobile boundaries; this could be due to loss of a long-range ordered ferroelectric phase or to a decrease in the volume fraction of micropolar regions. For the short range ordered PMN film, α goes through a similar peak, but the magnitude of α is smaller.

Figure 9 shows the thermal depolarization current density measured on heating under zero field conditions in the long range ordered PMN heterostructure films from 75 K-275 K. This shows the presence of depolarization temperature peak at ~125 K, which is in close agreement to the maximum in the irreversible Rayleigh coefficient. This peak would correspond to the discharge of the polarization developed during the prior field cooling on the sample, similar to field induced normal ferroelectric to relaxor phase transition in doped PMN ceramics[46]. The calculated polarization, obtained by integrating the area under the curve in the temperature range from 75 K-225 K was ~4.2 μC/cm$^2$. This low value may be attributed to the loss in polarization due to time dependent zero field aging, previously observed in PMN single crystals above 200 K[47,48]. The depolarization temperature at 125 K is much lower than that in undoped bulk PMN (~213 K), which may be partly attributed to 1% La doping of the $Pb_{1.2}Mg_{2/3}Nb_{1/3}O_{3.2}$ target; as demonstrated by Zhao et al[46].

### 2.3. Second harmonic generation (SHG) optical measurement and non linear higher harmonic measurement

Second harmonic generation measurement was used to further investigate the heterostructure films as a function of temperature. This technique does not require the application of electric fields,

This article is protected by copyright. All rights reserved.



Author Manuscript

eliminating the potential impact of the small signals used for dielectric characterization on nucleation of a long-range ordered ferroelectric phase. Figure 10 shows the SHG response for LSMO (bottom electrode), short range ordered PMN film and ordered PMN heterostructures during heating and cooling cycles. Compared to short range ordered PMN, the long-range ordered PMN films showed larger signals, suggesting an increased volume of a polar phase or larger nonlinear optical constant. Additionally, in the case of the PMN heterostructures, onset of features were consistently observed in the SHG data at 130 K during the heating cycle; the 130 K anomaly matches the temperature of the peak in the irreversible Rayleigh coefficient. This might indicate a change in ferroelectric ordering, due to the disruption of percolated domains (formed during the cooling cycle) with increasing temperature. Difference between the short range and the long range ordered PMN films, shown by the second harmonic and electrical characterization might imply difference in percolation of polar microdomain volume fractions, with increased ferroelectricity in the ordered case.

## 3. Conclusions

PMN is well studied relaxor ferroelectric perovskite, with coexistence of polar nano-regions, multivalent B site cation order in chemically ordered regions, and their intimate interactions in a paraelectric matrix. In undoped bulk PMN, the cation order can be hardly changed, though the polar order is responsive to both electric field and temperature. This work reports the first PMN thin film material with long-range cation order. Heterostructure films grown as alternate layers of $Pb(Mg_{2/3}Nb_{1/3})O_3$ and $PbNbO_3$ are compared to PMN films grown from a single target. It was found that the (111) orientation facilitated the phase pure growth of 111 ordered heterostructure films, compared to the (001) orientation. The heterostructures showed significantly larger regions of chemical ordering. Selected area electron diffraction confirmed emergence of superlattice spots

This article is protected by copyright. All rights reserved.



Author Manuscript

(1/2, 1/2, 1/2) with randomly distributed ordered domains as large as 100 nm. These heterostructures exhibited a dielectric constant of 800, loss tangents of approximately 0.03 and 2*remanent polarization of ~11 $\mu C/cm^2$ at room temperature. Polarization-electric field loops, Rayleigh data and optical second harmonic generation measurements are consistent with the development of ferroelectric domains below 140 K. The comparative study with short range ordered films elucidates the impact of long-range cation order in PMN on its electrical properties. Temperature dependent permittivity measurements demonstrate reduced frequency dispersion compared to short range ordered PMN films. It was observed that the relaxor behavior did not "switch "off" in the presence of longer range ordering along one axis, although the Rayleigh, polarization and thermal depolarization data are consistent with increased levels of longer-range ferroelectric ordering. This work is an important step towards addressing many scientific questions in relaxor ferroelectricity such as understanding the interaction between chemically ordered regions and the polar domains. It is anticipated that this work will be useful in refining the models for relaxor ferroelectric behavior as a function of chemical ordering. This could have technological significance on further improving usage of PMN based material properties for tunability applications.

## 4. Experimental Section

Prior to deposition, (001) and (111) $SrTiO_3$ substrates were prepared by chemical etching with a 50:1 buffered-oxide etchant (BHF) for 6 minutes, followed by a thermal anneal at 1273 K for 3 hours in order to achieve step-terrace structures for the step-flow/layer-by-layer growth of the bottom electrode. $La_{0.7}Sr_{0.3}MnO_3$ films (~45 nm thick) were epitaxially grown as the bottom electrode on the treated $SrTiO_3$ substrates by pulsed-laser deposition, employing a KrF excimer laser (248 nm; Coherent LPX305) from a ceramic $La_{0.7}Sr_{0.3}MnO_3$ target (Praxair Specialty Ceramics). The $La_{0.7}Sr_{0.3}MnO_3$ layer was deposited at 973 K in an oxygen pressure of 100 mTorr, with a laser

This article is protected by copyright. All rights reserved.



Author Manuscript

fluence of 1.5 J/cm$^2$ at a repetition rate of 5 Hz. Heterogeneous long range ordered PMN film growth was achieved via subsequent pulsing of the $Pb_{1.2}NbO_{3.2}$ and $Pb_{1.2}Mg_{2/3}Nb_{1/3}O_{3.2}$ targets doped with 1% La doped at 873 K in an oxygen pressure of 200 mTorr at a laser fluence of 0.75 J/cm$^2$ and a laser repetition rate of 3 Hz. Short range ordered $PbMg_{1/3}Nb_{2/3}O_3$ films were also grown from a single stoichiometric PMN target with 20% excess Pb, under similar growth conditions for comparison. Following growth, all samples were cooled to room temperature at a static oxygen pressure of 100 Torr. For clarity, the multi-target films are referred as long range ordered PMN heterostructures (LRO) while the single target films are referred as short range ordered PMN (SRO).+

The crystalline structure of the films was investigated by PANalytical 4-circle X'Pert 3 MRD X-ray diffractometer (XRD) with Cu Ka radiation (PANalytical B.V., Almelo, The Netherlands). 100-nm-thick platinum top electrodes were sputter deposited via a lift-off procedure for electrical characterization. Temperature-dependent structural characterization was achieved using a Gatan cooling in-situ holder (Model 613) on Titan3 dual aberration corrected scanning/TEM (S/TEM) operated at 200 kV. Room temperature selected area electron diffraction followed by dark-field imaging was used to identify the F-type ordering spot {h+1/2, k+1/2, l+1/2} and chemically-ordered domains for both long range ordered and short range ordered PMN samples, similar to the procedure employed in bulk samples[49]. In addition, the PNRs were imaged at the 111-fundamental reflection as a function of temperature (100-296 K) in the long range ordered PMN heterostructures. TEM specimens were prepared by *in situ* milling in a FEI Helios NanoLab DualBeam 660 focused-ion beam (FIB). Before milling, a thick protective amorphous carbon layer was deposited over the region of interest by electron-beam deposition. The FIB-TEM membrane was fabricated with a starting

Author Manuscript

This article is protected by copyright. All rights reserved.

milling voltage of 30 kV and then stepped down to 2 kV to minimize sidewall damage and thin the specimen to electron transparency.

Temperature dependent polarization- electric field hysteresis loops, small signal dielectric response, and the ac field dependence of the dielectric response were characterized using a cryo-cooled probe station (Lakeshore CRX-VF) from 10 -350 K. Prior to measurement, both long range ordered and short ordered samples were annealed at 723 K in a rapid thermal annealer for 1 min to erase any aging. The samples were subsequently zero field cooled to 10 K in the cryocooled probe station and the dielectric response was measured on heating. Polarization-electric field (P-E) hysteresis loops were measured at 10 kHz using a Multiferroic tester (Radiant Technology, Inc. Albuquerque, NM). The ac field and frequency dependence of the relative dielectric permittivity was characterized using an HP 4248A precision LCR meter (Agilent Technology, Palo Alto, CA) from 0.5-100 kHz. Thermal depolarization measurement was carried out on long range order PMN heterostructure film using a pA meter (HP 4140 B) during zero-field heating (heating rate of ~4 K/min) in the temperature range of 75-400 K. The sample has been previously cooled under an electric field of 200 kV/cm (cooling rate of ~1 K/min). Second harmonic generation measurements were conducted to verify the transition temperature and symmetry breaking without the application of an electric field. A Janis ST300 (Janis Research Company, Woburn, MA) temperature system with liquid nitrogen coolant was used to control the sample temperature during measurements. The samples were probed using a Solstice Ace (Spectra-Physics, Santa Clara, CA) femtosecond puled laser beam (100 fs, 1kHz) at a fundamental wavelength of 800 nm. The second harmonic signal (400 nm) was detected using a photomultiplier tube (Hamamatsu H7826, Hamamatsu, Japan) and a Stanford Research (Sunnyvale, CA) SR830 lock-in amplifier.

Author Manuscript

This article is protected by copyright. All rights reserved.

**Acknowledgements**

This work was funded by the Penn State MRSEC, Center for Nanoscale Science, under the award NSF DMR-1420620. The authors would also like to acknowledge the help of Beth Jones and Jeff Long in target preparation and electrical characterization setup. A.R.D. acknowledges support of the Army Research Office under Grant W911NF-14-1-0104. L.W.M. acknowledges support from the National Science Foundation under grant DMR-1708615.

Author Manuscript

References

[1] G. A. Smolensky, *J. Phys. Soc. Japan* **1970**, *28*, 26.

[2] L. E. Cross, *Ferroelectrics* **1994**, *151*, 305.

[3] S.-E. Park, T. R. Shrout, *J. Appl. Phys.* **1997**, *82*, 1804.

[4] F. Li, S. Zhang, T. Yang, Z. Xu, N. Zhang, G. Liu, J. Wang, J. Wang, Z. Cheng, Z. G. Ye, J. Luo, T. R. Shrout, L. Q. Chen, *Nat. Commun.* **2016**, *7*, 1.

[5] F. Li, S. Zhang, Z. Xu, L. Q. Chen, *Adv. Funct. Mater.* **2017**, *27*.

[6] N. Setter, L. E. Cross, *J. Appl. Phys.* **1980**, *51*, 4356.

[7] L. Cross, *Ferroelectrics* **1987**, *76*, 241.

[8] A. Bokov, Z.-G. Ye, *J. Mater. Sci.* **2006**, *41*, 31.

[9] D. Viehland, S. J. Jang, L. E. Cross, M. Wuttig, *J. Appl. Phys.* **1990**, *68*, 2916.

[10] A. Levstik, Z. Kutnjak, C. Filipič, R. Pirc, *Phys. Rev. B* **1998**, *57*, 11204.

[11] V. Westphal, W. Kleemann, G. M., *Phys. Rev. Lett.* **1992**, *68*, 847.

[12] A. Glazounov, A. K. Tagantsev, *Ferroelectrics* **1999**, *221*, 57.

[13] A. E. Glazounov, A. K. Tagantsev, *J. Phys. Condens. Matter* **1998**, *10*, 8863.

[14] W. Kleemann, *J. Mater. Sci.* **2006**, *41*, 129.

This article is protected by copyright. All rights reserved.

[15] W. Kleemann, *Phys. Status Solidi Basic Res.* **2014**, *251*, 1993.

[16] S. Hong, J. Woo, H. Shin, J. U. Jeon, Y. E. Pak, E. L. Colla, N. Setter, E. Kim, K. No, *J. Appl. Phys.* **2001**, *89*, 1377.

[17] X. Zhao, W. Qu, X. Tan, A. Bokov, Z.-G. Ye, *Phys. Rev. B* **2007**, *75*, 104106.

[18] E. V. Colla, E. Y. Koroleva, N. M. Okuneva, S. B. Vakhrushev, *Phys. Rev. Lett.* **1995**, *74*, 1681.

[19] C. Randall, A. Bhalla, *Jpn. J. Appl. Phys.* **1990**, *29*, 327.

[20] C. Randall, D. Barber, R. Whatmore, P. Groves, *J. Mater. Sci.* **1986**, *21*, 4456.

[21] M. A. Akbas, P. K. Davies, *J. Am. Ceram. Soc.* **1997**, *80*, 2933.

[22] M. A. Akbas, P. K. Davies, *J. Am. Ceram. Soc.* **2000**, *83*, 119.

[23] P. K. Davies, M. Akbas, *Ferroelectrics* **1999**, *221*, 27.

[24] P. K. Davies, L. Farber, M. Valant, M. A. Akbas, In *AIP Conference Proceedings*; 2000; Vol. 535, pp. 38–46.

[25] P. K. Davies, M. Akbas, *MRS Symp. Proc.* **1999**, *541*, 425.

[26] P. K. Davies, *J. Solid State Chem.* **2000**, *4*, 467.

[27] P. K. Davies, M. Akbas, *MRS Symp. Proc.* **1999**, *541*, 425.

[28] D. Fu, H. Taniguchi, M. Itoh, S. Y. Koshihara, N. Yamamoto, S. Mori, *Phys. Rev. Lett.* **2009**, *103*, 2.

[29] Y. Yan, S. J. Pennycook, Z. Xu, D. Viehland, *Appl. Phys. Lett.* **1998**, *72*, 3145.

[30] H. Z. Jin, J. Zhu, S. Miao, X. W. Zhang, Z. Y. Cheng, *J. Appl. Phys.* **2001**, *89*, 5048.

[31] R. A. Cowley, S. N. Gvasaliya, S. G. Lushnikov, B. Roessli, G. M. Rotaru, *Adv. Phys.* **2011**, *60*, 229.

[32] F. Chu, I. M. Reaney, N. Setter, *J. Am. Ceram. Soc.* **1995**, *78*, 1947.

[33] F. Chu, N. Setter, a. K. Tagantsev, *J. Appl. Phys.* **1993**, *74*, 5129.

[34] I. W. Chen, P. Li, Y. Wang, *J. Phys. Chem. Solids* **1996**, *57*, 1525.

[35] D. Viehland, S. J. Jang, L. E. Cross, M. Wuttig, *Phys. Rev. B* **1992**, *46*, 8003.

[36] B. P. Burton, E. Cockayne, S. Tinte, U. V Waghmare, *Phase Transitions* **2006**, *79*, 91.

Author Manuscript

This article is protected by copyright. All rights reserved.

[37] S. Wakimoto, C. Stock, Z.-G. Ye, W. Chen, P. M. Gehring, G. Shirane, *Phys. Rev. B* **2002**, *66*, 224102.

[38] M. Yoshida, S. Mori, N. Yamamoto, Y. Uesu, J. M. Kiat, *J. Korean Phys. Soc.* **1998**, *32*, 993.

[39] W. Qu, X. Zhao, X. Tan, *J. Appl. Phys.* **2007**, *102*, 0.

[40] E. Garboczi, K. Snyder, J. Douglas, M. Thorpe, *Phys. Rev. E* **1995**, *52*, 819.

[41] I.-K. Jeong, T. W. Darling, J. K. Lee, T. Proffen, R. H. Heffner, J. S. Park, K. S. Hong, W. Dmowski, T. Egami, *Phys. Rev. Lett.* **2005**, *94*, 147602.

[42] T. M. Shaw, S. Trolier-McKinstry, P. C. McIntyre, *Annu. Rev. Mater. Sci.* **2000**, *30*, 263.

[43] K. Lefki, G. J. M. Dormans, *J. Appl. Phys.* **1994**, *76*, 1764.

[44] M. J. Cabral, S. Zhang, E. C. Dickey, J. M. LeBeau, *Appl. Phys. Lett.* **2018**, *112*, 082901.

[45] A. K. Tagantsev, A. E. Glazounov, *Phase Transitions* **1998**, *65*, 117.

[46] X. Zhao, *Ph.D Diss.* **2008**.

[47] E. V. Colla, N. Jurik, Y. Liu, M. Delgado, M. Weissman, D. Viehland, Z.-G. Ye, *J. Appl. Phys.* **2013**, *184104*, 1.

[48] E. V. Colla, D. Vigil, J. Timmerwilke, M. B. Weissman, D. D. Viehland, B. Dkhil, *Phys. Rev. B - Condens. Matter Mater. Phys.* **2007**, *75*, 1.

[49] A. Hilton, C. Randall, D. Barber, T. Shrout, *Ferroelectrics* **1989**, *93*, 379.

Author Manuscript

This article is protected by copyright. All rights reserved.

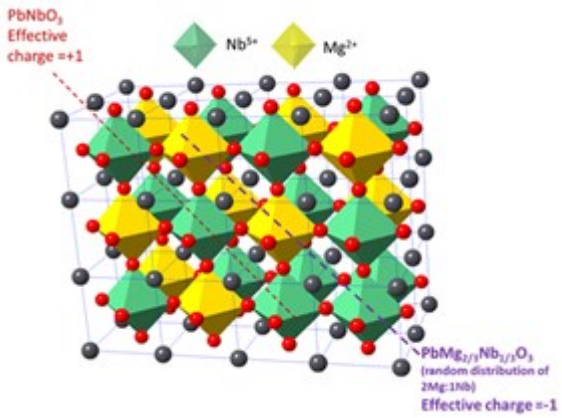


**Figure 1.** Proposed PMN heterostructure with alternate $PbNbO_3$ and $PbMg_{2/3}Nb_{1/3}O_3$ layering along <111>

Author Manuscript

This article is protected by copyright. All rights reserved.

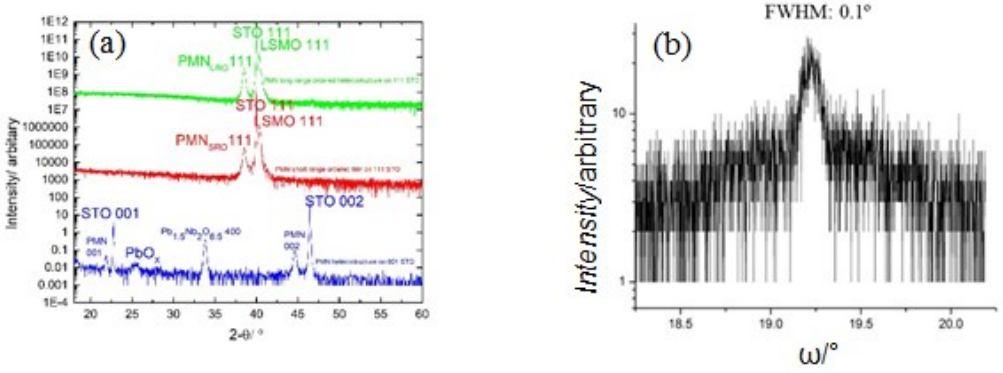


**Figure 2.** (a) XRD pattern for long range ordered PMN heterostructure film grown on 001 and 111 STO (labelled as $PMN_{LRO}$)and short range ordered PMN on 111 STO (labelled as $PMN_{SRO}$) (b) ω-scan for 111 reflection on 30 nm PMN heterostructure film grown on STO

Author Ma

This article is protected by copyright. All rights reserved.

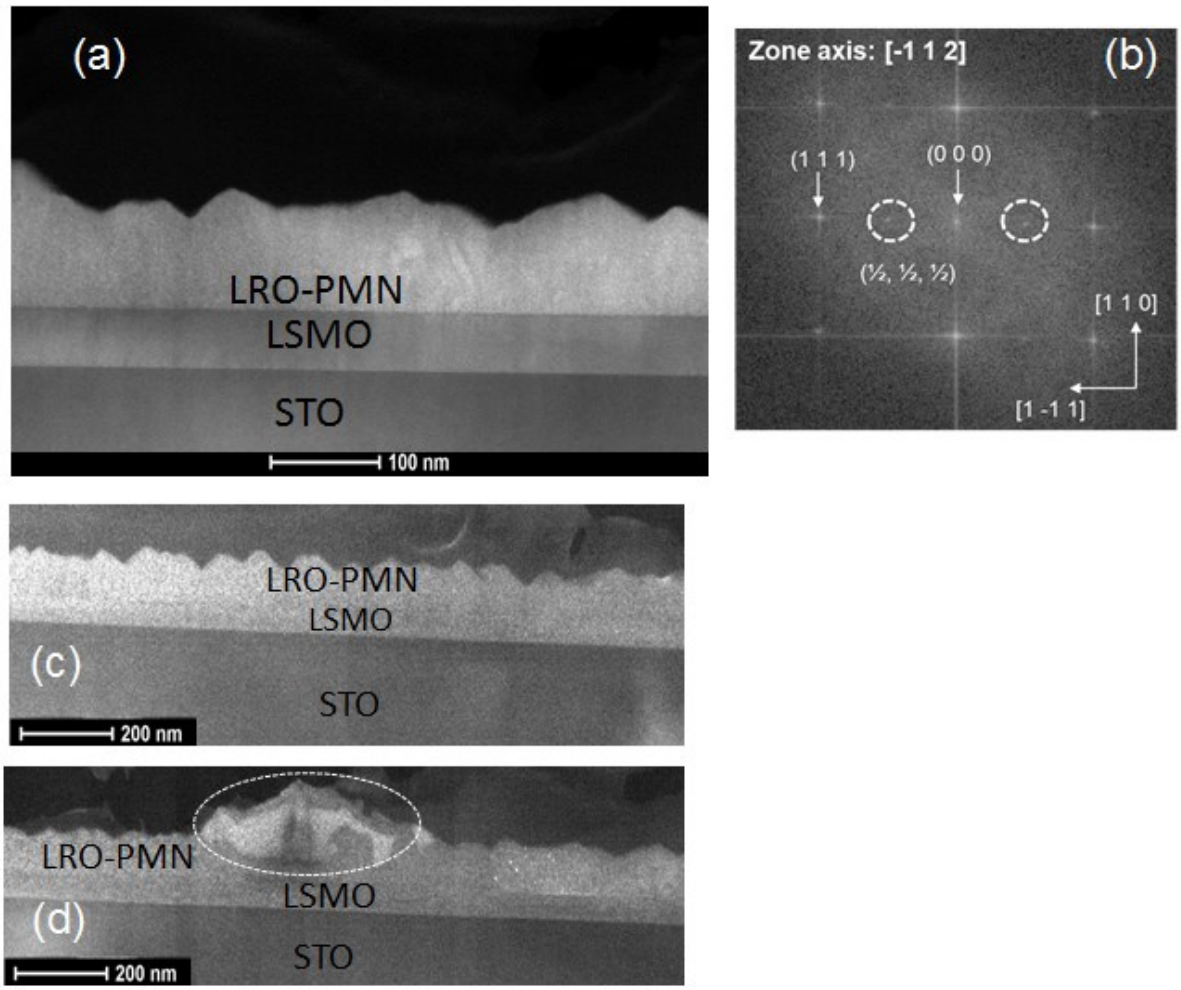


**Figure 3.** (a) A cross-section TEM image of a long range ordered heterostructure PMN (111) film (marked LRO-PMN) on LSMO/STO (111) recorded along the [−112] pole (b) FFT from a high resolution TEM image (INSET) showing superstructure reflections; (c)(d) cross-sectional dark field images captured using one of the superstructure reflections in (b), revealing the highlighted cation-ordered domain in the film.

This article is protected by copyright. All rights reserved.

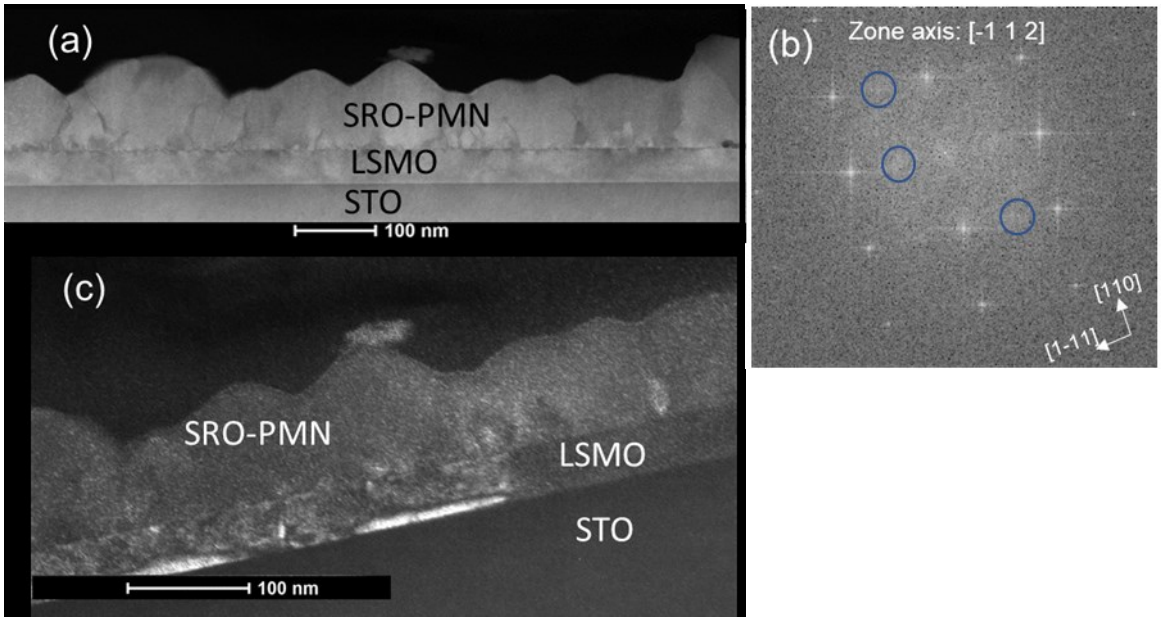


**Figure 4.** (a) A cross-section TEM image pattern of a short range ordered PMN (111) film (marked SRO-PMN) on LSMO/STO (111) (b) FFT of a high resolution TEM image recorded along the [−112] pole showing diffused superstructure reflections (marked by blue circles) associated with short-range cation ordering; (c) a cross-sectional dark field image captured using one of the superstructure reflections in (inset), revealing cation-ordered domains in the PMN film of a few tens of nm in size.

Author

This article is protected by copyright. All rights reserved.

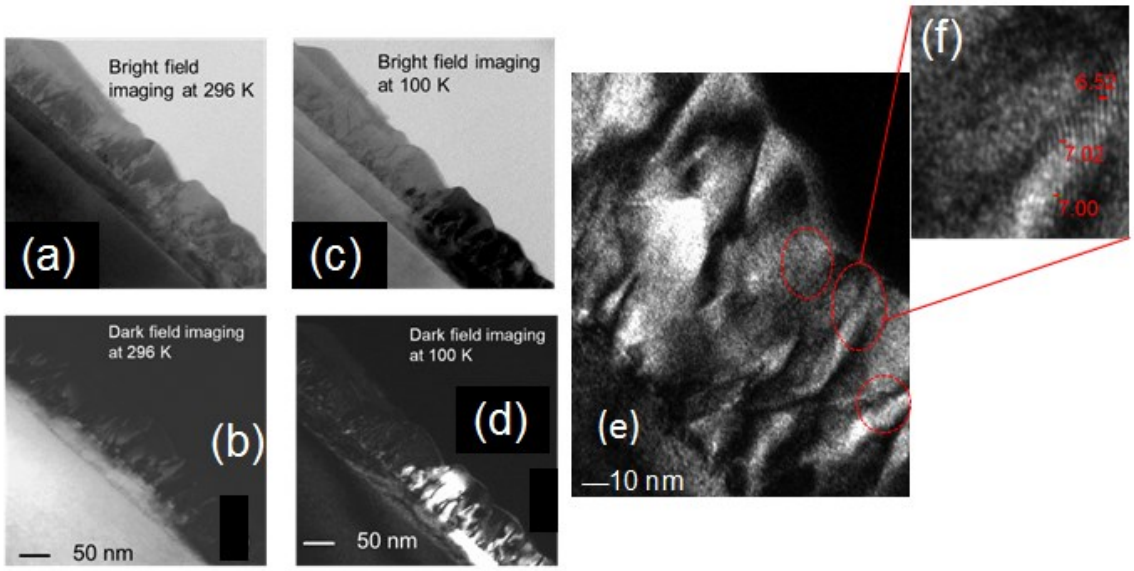


**Figure 5.** (a),(b) Cross-sectional bright and dark field TEM image of ordered heterostructure PMN (111) film on LSMO/STO (111) at 296 K (c),(d) A cross-section bright and dark field TEM image of or PMN (111) film on LSMO/STO (111) at 10 K, (e) A magnified dark field image (red circular regions show polar fringes) and (f) magnified image showing evidence of polar nanoregion striations through the film thickness with interfringe spacing of ~7 nm.

Author

This article is protected by copyright. All rights reserved.

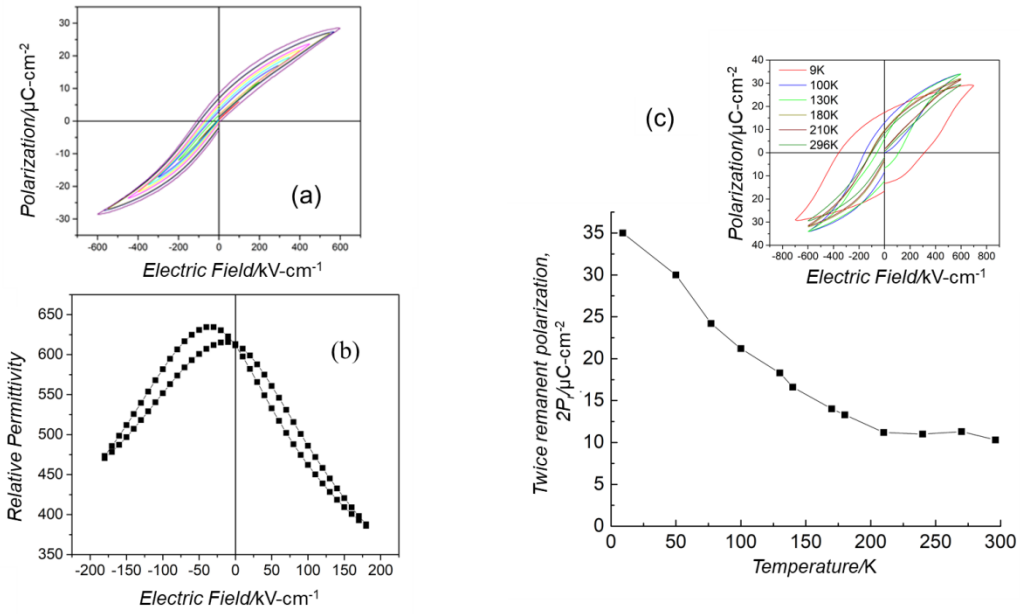


**Figure 6.** (a) Room temperature P-E loop evolution as a function of ac field; (b) permittivity field data at 10 kHz showing switching (c) Twice remanent polarization ($2P_r$) as a function of temperature with inset showing polarization evolution in long range ordered PMN heterostructure thin films at select temperatures

Author

This article is protected by copyright. All rights reserved.

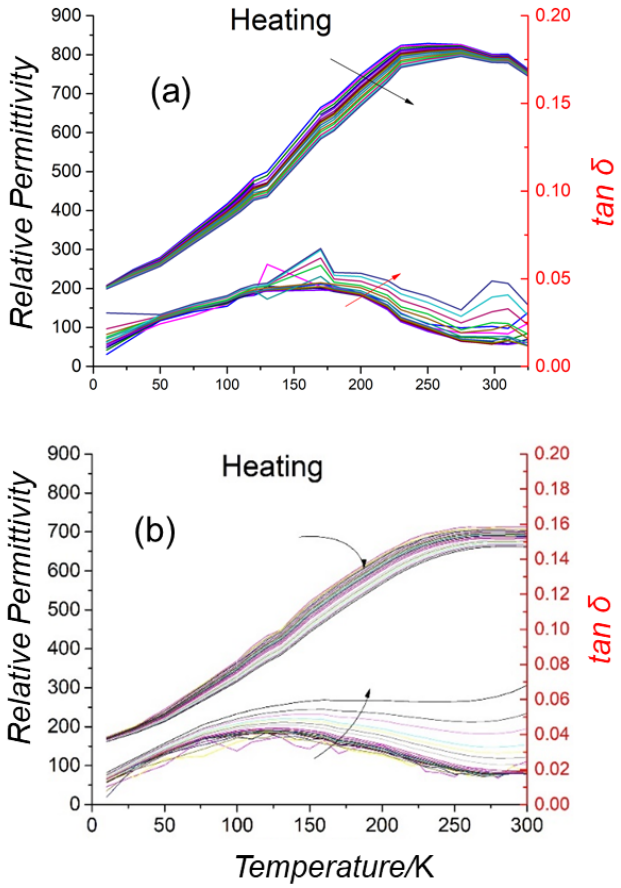


**Figure 7.** (a) Temperature dependence of dielectric response for long range ordered PMN films as a function of frequency during heating cycle (b) Temperature dependence of dielectric response for short range ordered PMN films as a function of frequency during heating cycle. Note arrows indicate increasing frequency (from ~ 1 kHz - ~ 300 kHz). In both cases, the upper set of curves correspond to the permittivity and the lower set of curves correspond to the loss tangent.

AU

This article is protected by copyright. All rights reserved.

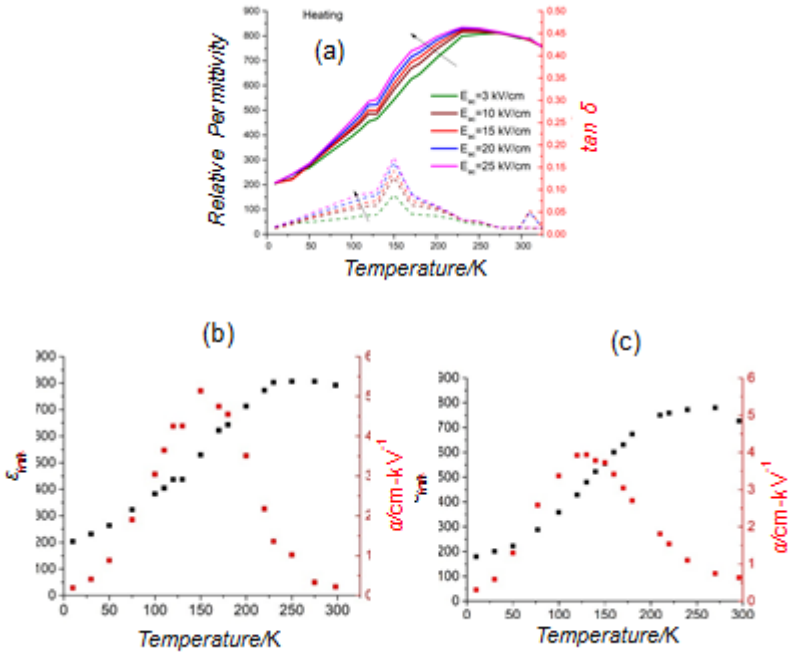


**Figure 8.** (a) Dielectric permittivity of ordered PMN as a function of ac field at 1kHz (b) Reversible and irreversible Rayleigh coefficients of the relative permittivity of a heterostructure PMN film as a function of temperature (c) Reversible and irreversible Rayleigh coefficients of the relative permittivity of a short range ordered PMN film as a function of temperature

Author

This article is protected by copyright. All rights reserved.

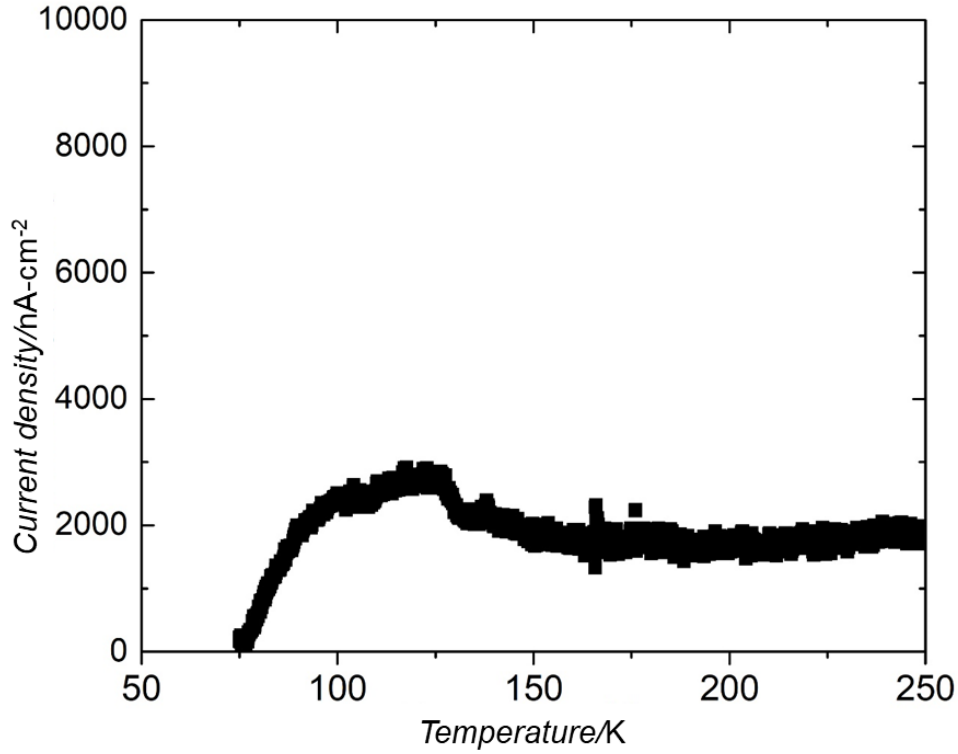


**Figure 9.** Depolarization current from long range ordered PMN on heating at E=0 KV/cm, after cooling at E=275 kV/cm, showing peak at 125 K.

This article is protected by copyright. All rights reserved.

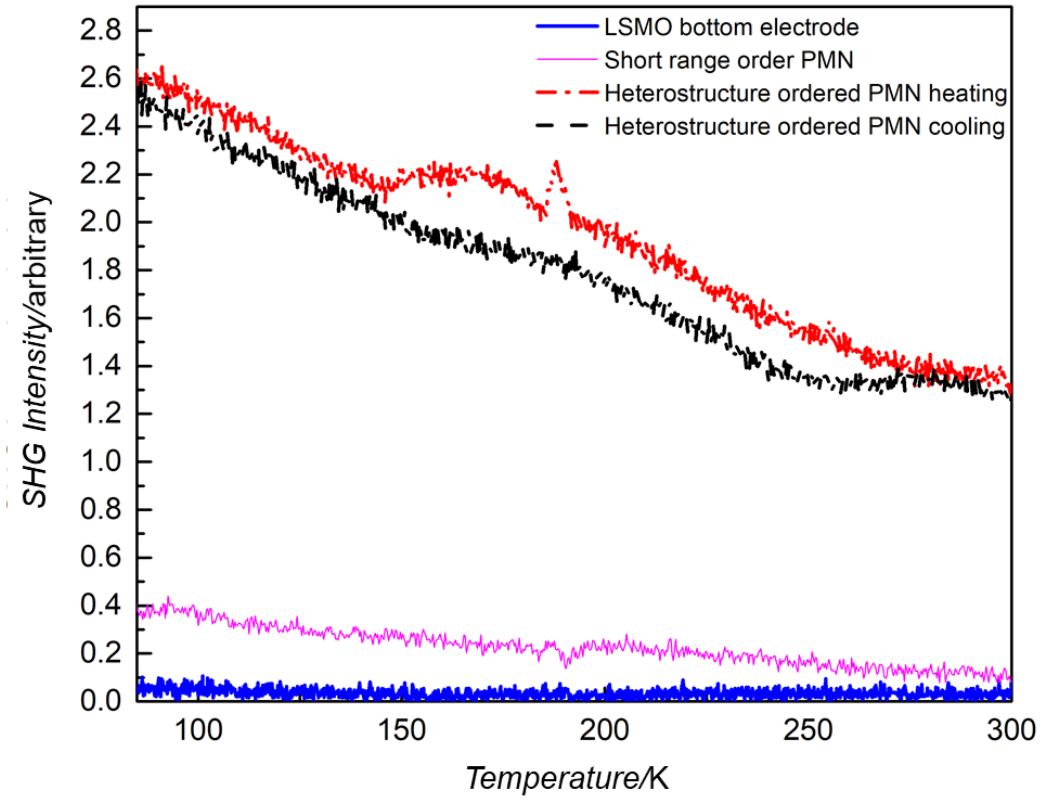


**Figure 10.** (a) Second harmonic generation results for LSMO on STO substrate, short range ordered PMN and long range ordered PMN heterostructure during heating and cooling cycles

Author

This article is protected by copyright. All rights reserved.

This work reports the first PMN ($PbMg_{1/3}Nb_{2/3}O_3$) thin film with long-range cation order via synthesis of heterostructures with alternate layers of $Pb(Mg_{2/3}Nb_{1/3})O_3$ and $PbNbO_3$, as suggested by the random-site model. The comparative study elucidates the impact of increased cation order in PMN on its characteristic relaxor ferroelectric behavior.

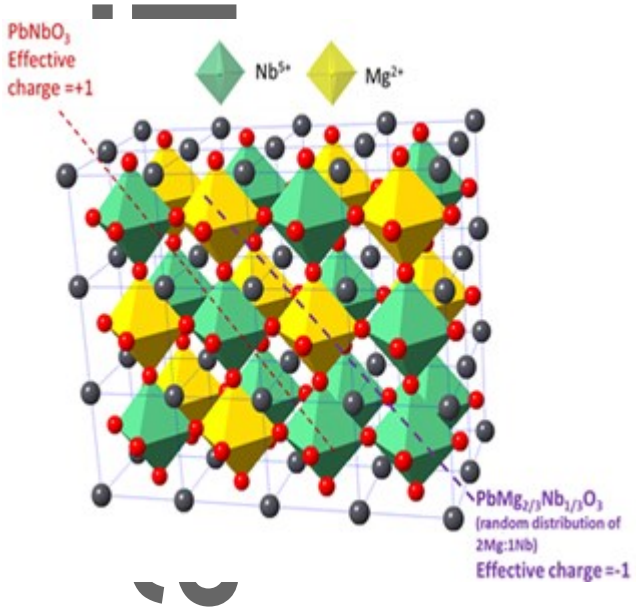


Author Manuscript

This article is protected by copyright. All rights reserved.